Selective Cell Adhesion and Biosensing Applications of Bio-Active Block Copolymers Prepared by CuAAC/Thiol-ene Double Click Reactions

Gizem Oyman Eyrilmez, Sean Doran, Eljesa Murtezi, Bilal Demir, Dilek Odaci Demirkol, Hakan Coskunol, Suna Timur,* Yusuf Yagci*

N-Acetyl-L-cysteine (NAC)-capped poly(methyl methacrylate)-*b*-polycaprolactone block copolymer (PMMA-*b*-PCL-NAC) was prepared using the previously described one-pot photo-induced sequential CuAAC/thiol-ene double click procedure. PMMA-*b*-PCL-NAC had previously shown good applicability as a matrix for cell adhesion of cells from the Vero cell line (African green monkey kidney epithelial). Here, in this work, PMMA-*b*-PCL-NAC served as an excellent immobilization matrix for biomolecule conjugation. Covalent binding of RGD (R: arginine, G: glycine, and D: aspartic acid) peptide sequence onto the PMMA-*b*-PCL-NAC-coated surface was performed via EDC chemistry. RGD-modified PMMA-*b*-PCL-NAC (PMMA-*b*-PCL-NAC-RGD) as a non-toxic cell proliferation platform was used for selective "integrin αvβ3-mediated cell adhesion and biosensing studies. Both optical and electrochemical techniques were used to monitor the adhesion differences between "integrin αvβ3" receptor positive and negative cell lines on to the designed biofunctional surfaces.

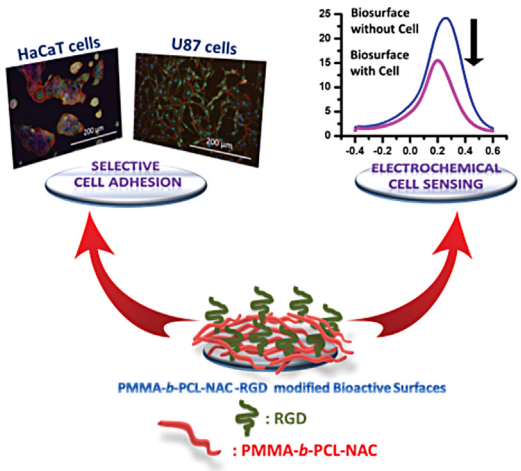

G. Oyman Eyrilmez
Department of Biotechnology, Graduate School of Natural and Applied Sciences, Ege University, 35100 Izmir, Turkey
S. Doran, E. Murtezi, Y. Yagci
Faculty of Science and Letters, Department of Chemistry, Istanbul Technical University, Maslak 34469 Istanbul, Turkey
S. Timur, B. Demir, D. Odaci Demirkol
Faculty of Science, Department of Biochemistry, Ege University, 35100 Izmir, Turkey

D. Odaci Demirkol, S. Timur
Institute on Drug Abuse, Toxicology and Pharmaceutical Science, Ege University, 35100 Izmir, Turkey
E-mail: suna.timur@ege.edu.tr
H. Coskunol
Faculty of Medicine, Psychiatry Department, Ege University, 35100 Izmir, Turkey
Y. Yagci
Faculty of Science, Chemistry Department, Center of Excellence for Advanced Materials Research (CEAMR), King Abdulaziz University, PO Box 80203, Jeddah 21589 Saudi Arabia
E-mail: yusuf@itu.edu.tr

[a] **Supporting Information** is available online from the Wiley Online Library or from the author.

1. Introduction

Cell-on-a-chip systems have a great importance because of their numerous advantageous such as increased sensitivity, continuous flow, and real time analysis.[1] Besides, these systems can be used to monitor cellular viability, cell adhesion and proliferation, drug toxicity, and electrochemical sensing.[2,3] For cell-on-a-chip, the improvement of the biocompatibility of cell culture materials is very important. Therefore, an enormous amount of research has been conducted toward the design of functional surfaces with increased sensitivity and biocompatibility.[4–7] Especially, biodegradable synthetic polymers such as polycaprolactone (PCL), poly(lactic acid) (PLA), and poly-(lactideco-glycotide) (PLGA) have been employed as scaffolds for organ tissue growth but they generally show poor cytocompatibility. The surface modification of these synthetic biocompatible polymers with specific functional groups and biomolecules has been shown to change their surface properties and improve cytocompatibility.[8] The use of so-called click chemistry is a very effective route for modification of polymeric and macromolecular structures and has become widespread. These transformations are very high yielding and highly modular giving rise to little or no side products without the need for column chromatography, among other favorable attributes.[9] Among the archetypal click reactions are included the copper catalyzed azide–alkyne cycloaddition (CuAAC)[10] and the thiol-ene reaction.[11] Both reactions have been successfully employed extensively in macromolecular modification[12] related to bioapplications.

Recently, our group took advantage of their favorable properties to employ them sequentially in a one-pot procedure under photochemical conditions to obtain N-acetyl-L-cysteine (NAC)-capped poly(methyl methacrylate)-*b*-polycaprolactone block copolymer (PMMA-*b*-PCL-NAC). [13] PMMA-*b*-PCL-NAC was employed as a matrix for cell adhesion of cells from the Vero cell line (African green monkey kidney epithelial) and showed cell proliferation comparable to commercially available cell culture plates. Recent years, there has been lots of studies about improving cell adhesion, proliferation, and viability on polymer-modified surfaces for cell-on-a chip systems.[14–16] Especially, extracellular matrix (ECM) proteins, such as fibronectin, collagen, and laminin-coated surfaces, have widespread usage due to the their role in the modulation of integrin-dependent cell adhesion.[17–19] Integrins are cell surface transmembrane proteins that interact with ECM molecules. They are formed from 19 α- and 8 β-subunits that are expressed in 25 different α/β heterodimeric combinations on the cell surface.[20,21] Also, integrin probes can be used for sensing of selectively adhered and proliferated cells. Particularly, integrin alpha V beta 3 (αvβ3) is an important receptor for ECM proteins via their RGD (R: arginine, G: glycine, and D: aspartic acid) peptide sequence. Although integrin αvβ3 is poorly expressed in most healthy cells, it is highly expressed in many tumors.[22–28] Therefore, integrin αvβ3 is an interesting biological target for cancer treatment, imaging, and also sensing.[29]

Researchers have developed numerous surfaces to investigate integrin-mediated cell adhesion and proliferation.[30–33] Recently, researchers have worked toward improving new electrochemical cell-sensing surfaces for cell-on-a-chip systems. With this goal in mind, several cell detection based electrochemical methods have appeared mostly using mammalian cells, especially cancerous cell lines.[34] Normally, self-assembled modification of electrode surfaces have been used for bio-recognition of the relevant cell line. On the other hand, novel nanocomposite and/or polymeric adhesive materials could be attributed to this kind of approach. In our previous work, folic acid and poly(caprolactone)-modified clay nanocomposite were used in the selective cell attachment of folic acid overexpressed HeLa (ovarian cancer cell line) cells against A549 (lung cancer cell line). [5] Here, PMMA-*b*-PCL-NAC was synthesized according to the procedure published previously.[13] PMMA-*b*-PCL-NAC served as an excellent immobilization matrix for RGD modification. Introduction of RGD onto the PMMA-*b*-PCL-NAC-coated surface was performed through covalent binding using the well-established two-step carbodiimide coupling method.[35] Briefly, RGD-modified PMMA-*b*-PCL-NAC (PMMA-*b*-PCL-NAC-RGD) was successfully used as a targeted surface for cell culture applications to discriminate the proliferation behaviors of integrin αvβ3 receptor positive (U87-MG) and negative (HaCaT) cell lines.

2. Experimental Section

2.1. Materials

RGD peptide, EDC (1-ethyl-3-(3-dimethylaminopropyl) carbodiimide), Triton X-100, formaldehyde (37.0%), 4, 6-diamino-2-phenylindol (DAPI) were purchased from Sigma. THF (tetrahydrofuran), phosphate-buffered saline (pH 7.4, PBS) which was prepared using 8.0 $g \cdot L^{-1}$ NaCl, 0.2 $g \cdot L^{-1}$ KCl, 1.4 $g \cdot L^{-1}$ $Na_2HPO_4.2H_20$, and 0.2 g KH_2PO_4 were obtained from Merck. NAC end-capped PMMA-*b*-PCL-NAC was prepared as previously described.[13]

Dulbecco's modified Eagle medium (DMEM), Eagle's minimum essential medium (EMEM), fetal bovine serum (FBS), penicillin/streptomycin (P/S) (10 000/10 000 units), and 200 mM L-glutamine were purchased from Lonza. CytoPainter Phalloidin-iFluor 555 reagent, Anti-Integrin alpha V beta 3 (αvβ3) antibody (ab78289), and Goat Anti-Mouse IgG H&L (Alexa Fluor 488) (ab150117) were purchased from Abcam.

FT-IR spectra were recorded on Perkin–Elmer FT-IR spectrum one spectrometer with an ATR Accessory (ZnSe, PikeMiracle Accessory) and cadmium telluride (MCT) detector. Resolution was 4 cm^{-1} and

Macromolecular Journals

Macromol. Biosci. **2015,** DOI: 10.1002/mabi.201500099

24 scans with 0.2 cm $\cdot s^{-1}$ scan speed. A Philips XL-30S FEG model SEM was used. SEM analyses were carried out at 5.0 kV and 50 000× magnifications.

2.2. Cell Culture Studies

U87-MG (ATCC) and HaCaT (CLS) cell lines were maintained in EMEM and DMEM, respectively. Both of them supplemented with 10.0% FBS, and 1.0% P/S at 37 °C in a humidified incubator with 5.0% CO_2 in air. All cells were sub-cultured at 80% confluency by trypsinization every 2 or 3 d.

The expression of integrin αvβ3 in U87-MG cells and the lack of expression in HaCaT as a control cell line were confirmed by flow cytometry analyses. For flow cytometry studies, cells were harvested and washed once in cold PBS and in incubation buffer consisting of PBS supplemented with 2.0% FBS. After suspending in incubation buffer, 1×10^6 cells were collected and centrifuged. For cell staining, 2.0 μg Anti-Integrin αvβ3 antibody was added and incubated at room temperature for 1 h. Negative control staining was performed using matched mouse IgG1, isotype control antibody (BD Biosciences, Heidelberg). After then, secondary staining was performed by using Goat Anti-Mouse IgG H&L (Alexa Fluor 488) antibody (1:2 000). Unbound antibodies were removed by washing three times in 1.0 mL incubation buffer. Immediately before flow cytometry analysis cells were suspended in 1.0 mL incubation buffer and then analyzed in a BD FACS flow cytometer. 10 000 gated events were observed in total and the living cells were gated in a dot plot of forward versus side scatter signals. For drawing dot plots FlowJo software (Tree Star, San Carlos, CA) was used.

PMMA-*b*-PCL-NAC and PMMA-*b*-PCL-NAC-RGD were compared to the commercial PS cell culture plates to observe their properties as cell culture materials. Thus, 0.5 mg $\cdot mL^{-1}$ PMMA-*b*-PCL-NAC (in 5.0% THF) was added into polystyrene-coated 96-well plates. Plates were dried for 72 h at room temperatures. To activate carboxyl groups of PMMA-*b*-PCL-NAC, 0.2 M EDC (in pH 7.4 PBS) were added into plates and incubated for 15 min. Then, PMMA-*b*-PCL-NAC-coated plates were incubated with 0.05 mg $\cdot mL^{-1}$ RGD peptide overnight and rinsed with PBS three times to remove unbound molecules. Afterward, the resulting PMMA-*b*-PCL-NAC-RGD-coated plates were sterilized under UV radiation for 15 min and used for the cell culture experiments. All coating experiments were performed at ambient temperature.

To observe time-dependent cellular viability, cells were incubated for 4, 24, 48, and 72 h on PMMA-*b*-PCL-NAC, PMMA-*b*-PCL-NAC-RGD, and also unmodified polystyrene-coated plates (PS). At the end of each cultivation time, cells were treated with 0.5 mg $\cdot mL^{-1}$ MTT (3-(4, 5-dimethylthiazol-2-yl)-2,5-diphenyltetrazolium bromide) for 4 h. Then, 10.0% of SDS (in HCl) was added per well and incubated overnight. Then, UV−vis absorption was measured at 570 nm with 630 nm as reference wavelength using a microplate reader (Bio-Tek Instruments, Inc., Winooski, VT). The conventional PS surface was used as control for each experiment.

HaCaT and U87 MG cells were cultured during 72 h to compare their proliferation behaviors on surfaces. CytoPainter Phalloidin-iFluor 555 Reagent and anti-integrin αvβ3 antibody were used to stain F-actin filaments and integrin transmembrane proteins of cells, respectively. For immunofluorescence staining, cells were fixed with 4.0% formaldehyde in PBS for 30 min at 37 °C after 72 h incubation times on surfaces. Permeabilization of cells was facilitated by treatment with 0.1% Triton X-100 for 4 min. Then, cells were stained for actin and integrin αvβ3 using CytoPainter Phalloidin-iFluor 555 Reagent (1:1 000) and anti-integrin αvβ3 antibody (1:500), followed by Alexa 488 fluorophore-conjugated secondary antibody (1:500). Also, DAPI (1.0 mg $\cdot mL^{-1}$) staining was performed at ambient temperature during 5 min. After extensive washing with PBS, the cells were imaged using an Olympus CKX71 fluorescence microscope with a 20× objective. The cell number was quantified for each surface by using Image J (NIH) software.

2.3. Construction of Electrochemical Cell-Sensing Platform

The glassy carbon electrodes (GCEs) were first polished using a piece of cloth with various sized alumina slurry, rinsed with distilled water, and then sonicated for 5 min in ethanol: distilled water to remove any substances on the electrode surface. During all the electrochemical measurements, a three electrode cell with GCE as the working electrode, Ag/AgCl electrode with 3.0 M KCl as a reference electrode and platinum (Pt) as the counter electrode were used equipped with PalmSens Potentiostat (Palm Instruments, Houten, the Netherlands). In order to construct the biosensor surface for the electrochemical cell sensing, initially 0.5 mg PMMA-*b*-PCL-NAC was dissolved in 100 μL THF and 900 μL PBS pH 7.4, and then 15 μL of this mixture was dropped onto the mirror-like GCE surface. After drying, the surface was treated with 0.2 M EDC (prepared in PBS, pH 7.4) for 15 min in order to activate –COOH groups. Subsequently, the electrode was rinsed with distilled water, and then 50 μL of RGD tripeptide (0.05 mg $\cdot mL^{-1}$ in PBS pH 7.4) was dropped to the modified electrode. Afterward, the electrode was allowed to stand for 1 h to generate a covalent bond between –COOH groups of PMMA-*b*-PCL-NAC and $-NH_2$ functionality of RGD peptide. At the final step, RGD-modified GCE surfaces were treated with different concentrations of cells for 2 h at ambient conditions (both glioblastoma (U87-MG as integrin αvβ3 receptor overexpressed cell line) and healthy keratinocyte (HaCaT- as negative control) were tested for the selective binding). Monitoring of the cell-binding capacity of bioactive surface was determined by using differential pulse voltammetry (DPV) and cyclic voltammetry (CV) techniques.

CV (between −0.4 and −0.8 V) and DPV (between −0.2 and −0.6 V) techniques were performed after each modification using $[Fe(CN)_6]^{3-/4-}$ as a water soluble redox probe (10 mM). Cell binding to the surface caused a decrease in DPV signals which were correlated with the cell loaded onto the surface. Differences between the current signals were calculated as follows:

$$\Delta I = \mathrm{Io} - \mathrm{Ic}$$

where Io is the mean current at zero cell concentration and Ic is the mean current at any concentration after cell binding onto the PMMA-*b*-PCL-NAC-RGD-covered surfaces.

2.4. Statistical Analysis

GraphPad Prism version 5.03 software (GraphPad Software, San Diego, CA) was used to obtain graphs and for statistical analyses. The non-parametric Mann–Whitney U-test was used to compare

relative cell numbers per surface area among different surfaces. Statistical significance was denoted with *, **, and *** for $p \leq 0.05$, $p \leq 0.01$, and $p \leq 0.001$, respectively.

3. Results and Discussion

The NAC end- PMMA-*b*-PCL-NAC was prepared using the photo-induced sequential copper-catalyzed azide–alkyne cycloaddition (CuAAC)/thiol-ene double-click procedure, as described previously. Bromo end-functional poly(methyl methacrylate) (PMMA) was prepared using standard atom transfer radical polymerization.[36] It was subsequently azidated under standard azidation conditions using sodium azide to afford PMMA with terminal azide functionality (PMMA-N_3). PCL was prepared along standard ring-opening polymerization (ROP) guidelines. The ROP of ε-caprolactone was initiated by propargyl alcohol, catalyzed by stannous octoate to afford a propargyl group functionalized polycaprolactone, α-hydroxyl–alkyne–poly(ε-caprolactone) (A-PCL).[37,38] A-PCL was then esterified with methacrylic acid through the Mitsonobu reaction to afford α-methacrylate–ω-alkyne–poly(ε-caprolactone) (A-PCL-MA).[38] With the precursors in hand, using the photo-induced one-pot sequential double-click procedure, PMMA-N_3 and A-PCL-MA were first clicked together through the CuAAC click reaction. Thereafter, in the same pot, NAC was clicked via the thiol-ene click to afford PMMA-*b*-PCL-NAC (Scheme 1).

The synthesized PMMA-*b*-PCL-NAC block copolymer was then modified with RGD peptide to provide integrin αvβ3-mediated cell sensing. RGD immobilization onto the PMMA-*b*-PCL-NAC block copolymer was performed via EDC cross-linking reaction (Scheme 2).

3.1. Characterization of RGD Binding

Analysis of FT-IR was used to confirm the incorporation of the RGD peptide onto the PMMA-PCL-NAC block copolymer, which can be observed in Figure 1. In the region between 1 550 and 1 650 cm^{-1}, two peaks can be observed in the IR

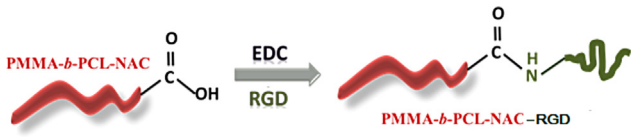

Scheme 2. Amide bond formation via EDC cross-linking between RGD (–NH_2) and PMMA-b-PCL-NAC (–COOH).

spectrum which correspond to the bending frequencies of the guanidine group present on the side chain of the l-arginine amino acid of the RGD peptide. Also at 2 916 cm^{-1}, the alkane stretching frequencies pertaining to the l-arginine amino acid side chain can be observed, thus confirming the presence of the RGD peptide.

Surface morphologies before (Figure S1) and after (Figure 2) RGD immobilization were examined by SEM. After the functionalization of PMMA-*b*-PCL-NAC surface, morphological changes cannot be observed well due to the small size of the RGD peptide.

Besides, voltammetry methods that include DPV and CV were applied during the measurements in the presence of ferricyanide as a redox probe. Hence, both methods were conducted to characterize the PMMA-*b*-PCL-NAC-RGD-modified electrode. Figure 3 illustrates the CV and DPV diagrams of the each modification step gradually. Following the PMMA-*b*-PCL-NAC-modified GCE, the oxidation and reduction peaks of the relevant voltammogram were decreased relative to the bare electrode. Subsequently, the –COOH group was activated by EDC reagent, and this activation enabled the formation of the amide bond between the carboxyl and amine (–NH_2) groups of the RGD peptide. This linkage was also evidenced in both CV and DPV by the increase of the redox peaks of the voltammograms due to the stronger attraction between the positively charged guanidino group of arginine (R) and the negatively charged *d* $[Fe(CN)_6]$ on the electrode surface. The general electrochemical characteristic for the modification of GCE due to integrin overexpressed U87 cell binding is demonstrated in Figure 3. As can be seen from the figure, the peak current values were assessed as 60.4 μA ($Ep_c = 0.33$ V) for bare GCE, 46 μA ($Ep_c = 0.37$ V) for the GCE/PMMA-*b*-PCL-NAC,

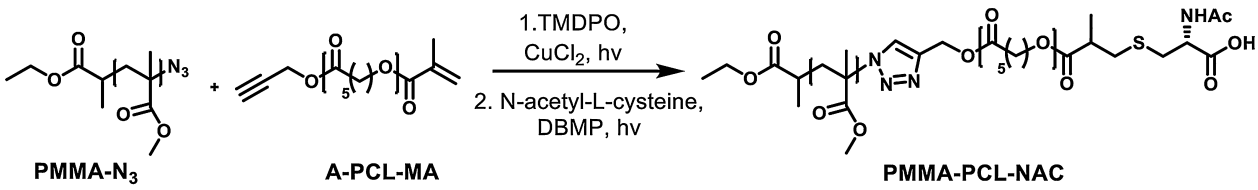

Photoinitiators
TMDPO = (2,4,6-trimethylbenzoyl)-diphenylphosphine oxide
DBMP = 2-benzyl-2-dimethylamino-4'-morpholinobutyrophenone

Scheme 1. Photo CuAAC/thiol-ene double click reaction to afford PMMA-PCL-NAC.

Macromolecular Journals

Macromol. Biosci. **2015,** DOI: 10.1002/mabi.201500099

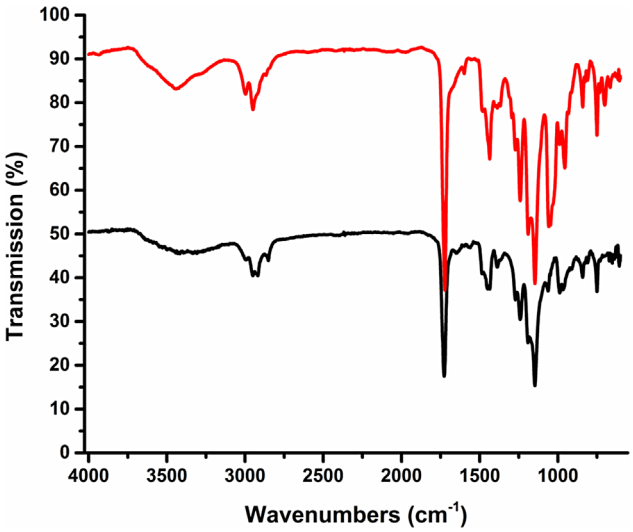

Figure 1. FT-IR spectra of the PMMA-*b*-PCL-NAC (red), and PMMA-*b*-PCL-NAC-RGD (black).

47 μA ($Ep_c = 0.36$ V) for the GCE/ PMMA-*b*-PCL-NAC-RGD, and 36.6 μA ($Ep_c = 0.36$ V) for the GCE/PMMA-*b*-PCL-NAC-RGD /U87–MG in the CV experiments. Moreover, to achieve a detailed and more quantitative result, DPV technique showed the detailed data about the modification of the electrode surface as the following peak current values: 35.4 μA (Ep = 0.22 V) for the GCE, 22.5 μA (Ep = 0.24 V) for the GCE/ PMMA-*b*-PCL-NAC, 23.7 μA (Ep = 0.23 V) for the GCE/ PMMA-*b*-PCL-NAC/RGD, and 14.7 μA (Ep = 0.18 V) for the GCE/ PMMA-*b*-PCL-NAC /RGD/U87-MG.

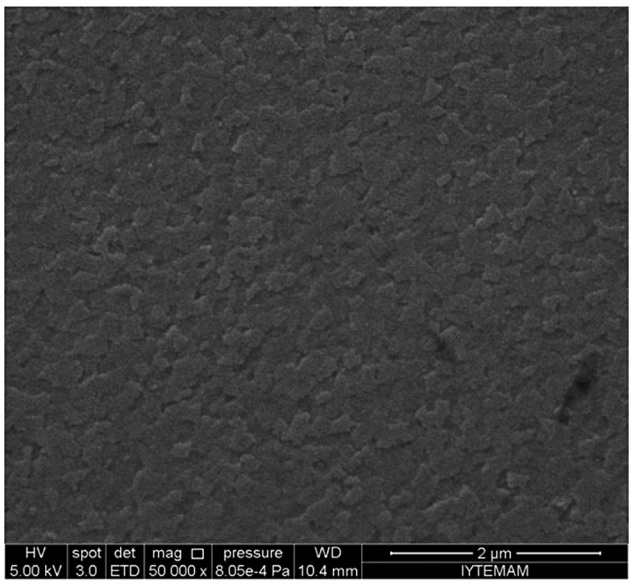

Figure 2. SEM image of PMMA-*b*-PCL-NAC-RGD surface (with 50 000× magnification).

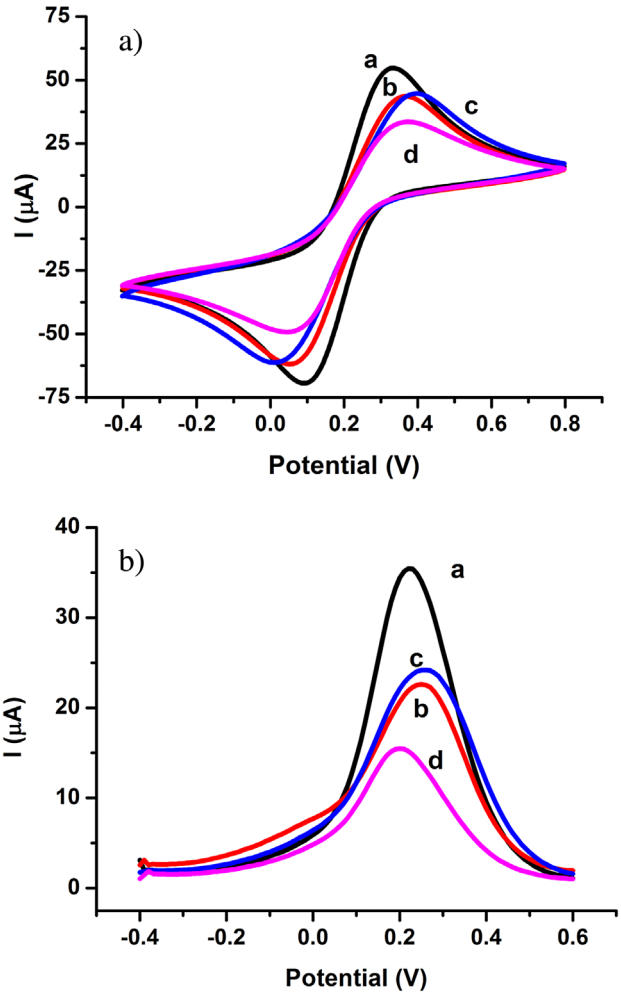

Figure 3. CV (A) and DPV (B) diagrams of (a) bare GCE, (b) GCE/ PMMA-*b*-PCL-NAC, (c) GCE/PMMA-*b*-PCL-NAC-RGD, (d) GCE/ PMMA-*b*-PCL-NAC-RGD/U87-MG (1.0×10^5 cells · mL^{-1}) (in the presence of 10.0 mM $[Fe(CN)_6]^{3-/4-}$ in PBS pH 7.4 under ambient conditions).

3.1.1. Cell Proliferation and Sensing

For the application of PMMA-*b*-PCL-NAC as a potential cell culture material with integrin-mediated cell adhesions, cells have to be characterized for their expression level of integrin αvβ3. Therefore, the fluorescence intensity of integrin αvβ3 was determined by flow cytometry. After cell staining, fluorescence intensity of each cell sample was read out separately and a dot plot graph of more than 10 000 gated cells were drawn (Figure 4). Each partial image shows a combination of cell staining using mouse IgG1-negative control (black line) and anti-human integrin αvβ3 (red line). Figure 4a and b illustrates the flow cytometry results of HaCaT and U87-MG cell lines, respectively. The median fluorescence intensity (MFI) of an anti-human integrin αvβ3-488 antibody staining (2 368) is almost identical to

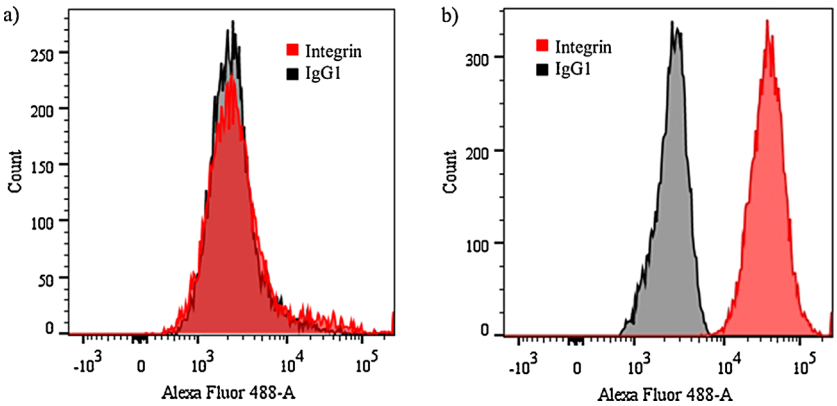

Figure 4. Plots of cell characterization for integrin αvβ3 expression via flow cytometry of HaCaT (a) and U87-MG (b); black plot: cells incubated with IgG1–Alexa Fluor 488 antibodies as a negative control, red plot: cells stained with anti-human integrin αvβ3-Alexa Fluor 488.

the intensity of IgG1-488 antibody (2 457) for HaCaT cell line. But for U87-MG cell line, 2 697 and 31 169 MFI was observed for lgG1 and integrin αvβ3, respectively. The integrin αvβ3 differences on the U87-MG cell surfaces can be clearly seen. According to the flow cytometry results, overexpression of integrin αvβ3 in U87-MG cells are proved as already reported in the literature.[39–41]

After integrin αvβ3 expression confirmation, time-dependent cellular viability on PMMA-*b*-PCL-NAC-RGD and PMMA-*b*-PCL-NAC surfaces was investigated by MTT assay. According to the results, cellular viability increases after RGD functionalization for both of the cell lines (Figure 5). Although cellular viability of HaCaT cells on PMMA-*b*-PCL-NAC-RGD is better than on PMMA-*b*-PCL-NAC, it is not good as commercial PS plates (Figure 5a). Moreover, increasing cellular viability of U87-MG cells was observed on RGD functionalized surfaces as much as commercial PS plates (Figure 5b). On the PMMA-*b*-PCL-NAC-RGD surfaces, U87-MG cells showed better growth behavior than HaCaT cells due to the presence of RGD peptide. We assume that the main reason for better growth behaviors of U87-MG cells is the presence of overexpressed integrin αvβ3 which interacts with RGD peptide sequence.

The effects of surface modification on the behaviors of U87-MG and HaCaT cell lines were investigated on commercial PS, PMMA-*b*-PCL-NAC and PMMA-*b*-PCL-NAC-RGD surfaces. Figure 6 shows that both of the cell lines attach and spread on the RGD functionalized surface to a greater extent than the unmodified PMMA-*b*-PCL-NAC block copolymer-coated surface. However, increased number of cells was observed on RGD functionalized surfaces for U87-MG cells due to the overexpression of integrin αvβ3 on this cell line.

The relationship between the average number of cells per mm^2 and both of the cell lines is shown in Figure 7. Higher cell number was observed on the PMMA-*b*-PCL-NAC-RGD surfaces than control and polymer-coated surfaces. The spreading of U87-MG cell line on the RGD-modified surfaces indicates that the cells interact with the RGD motif in an integrin-dependent manner.

According to the results, the increased number of U87-MG glioblastoma cells on the PMMA-*b*-PCL-NAC-RGD surfaces indicates that the cells selectively interact with the RGD peptide sequence that was immobilized on the block copolymer surface. After the investigation of cell-adhesive properties of the generated PMMA-*b*-PCL-NAC-RGD-modified surface, a similar

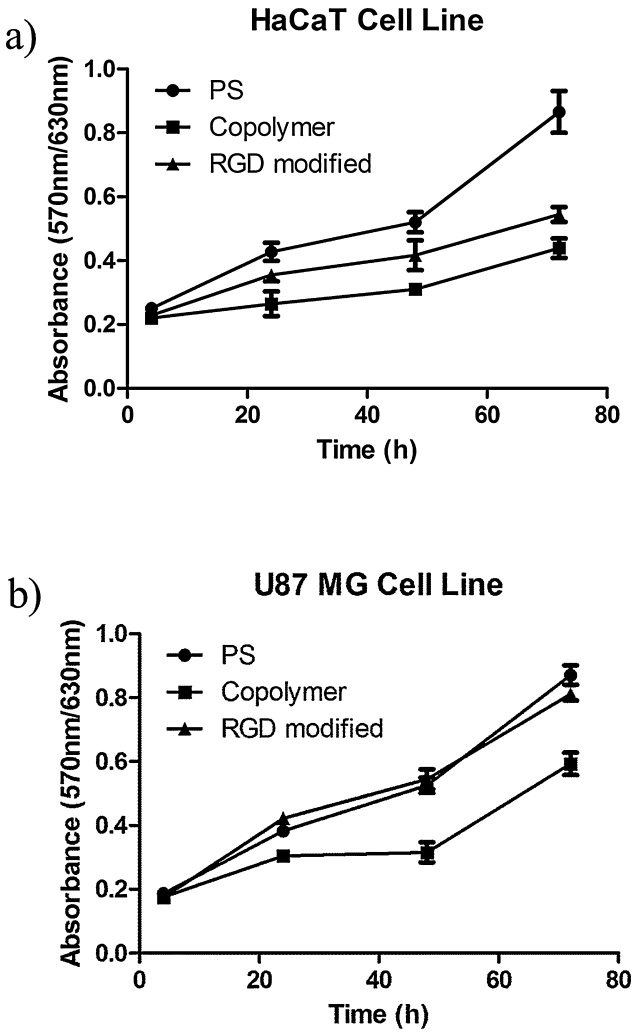

Figure 5. Time-dependent cellular viability of (a) HaCaT and (b) U87-MG cell lines on the commercial PS plates, PMMA-*b*-PCL-NAC and PMMA-*b*-PCL-NAC-RGD-modified surfaces. Error bars mean the ± SD ($n = 6$).

Macromol. Biosci. 2015, DOI: 10.1002/mabi.201500099

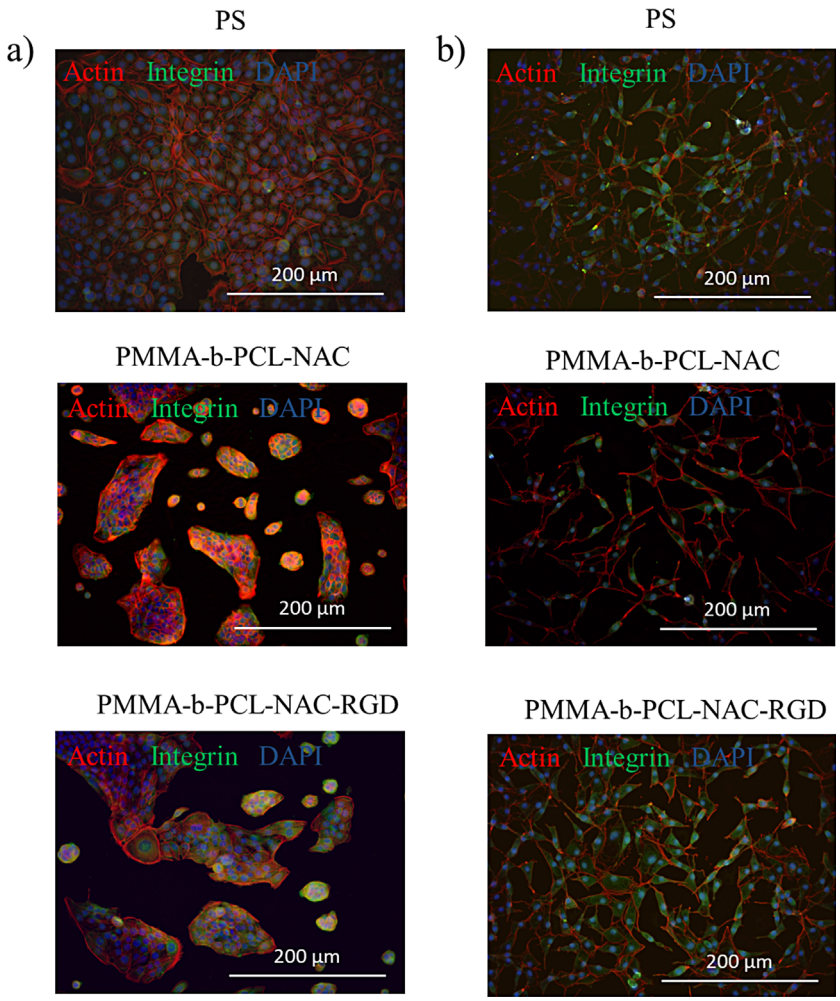

Figure 6. Proliferation behaviors of (a) HaCaT and (b) U87-MG cell lines after 72 h incubation on the commercial PS plates, PMMA-*b*-PCL-NAC and PMMA-*b*-PCL-NAC-RGD surfaces. Actin (red), integrin (green), and DAPI (blue) staining were performed. Scale bar: 200 µm.

procedure for cell-sensing studies was applied by modifying PMMA-*b*-PCL-NAC adsorption onto GCE prior to RGD linking via EDC chemistry. U87-MG glioblastoma cells and HaCaT keratinocytes were added to the peptide-modified GCE as positive and negative controls, respectively. In the manner of integrin $\alpha_v\beta_3$ receptor overexpression, integrin-RGD interaction can provide the selectivity against low expressed integrins on the cell surface. Thus, U87 cells exhibited linearity between 10 and 10^5 cells $\cdot mL^{-1}$ with high current differences and an equation which was defined as $y = 1.59x + 1.02$ ($R^2 = 0.994$). HaCaT keratinocytes did not show an effective binding onto the electrode surface and display linearity between 10^2 and 10^5 cells $\cdot mL^{-1}$ with lower current differences and an equation which was defined as $y = 0.82x - 0.332$ ($R^2 = 0.984$) (Figure 8). Besides, the detection limits of the sensor systems are 4.0 and 66.0 cells $\cdot mL^{-1}$ for U87-MG and HaCaT cell lines, respectively.

Under the light of these findings, it can be claimed that GCE/ PMMA-*b*-PCL-NAC-RGD biofilm could detect integrin overexpressed cell line by creating a selective attachment to the modified transducer. On the other hand, the developed affinity-type cell sensor may pave the way for those kinds of polymers to be applied in biosensing technologies and arrive at "cell-on-chip" applications rapidly.

4. Conclusion

In conclusion, a promising material that allows selective cell adhesion and proliferation was used as a cell culture and biosensing platform. Besides, it provides the best way for the detection of integrin $\alpha v\beta 3$ overexpressed cells via electrochemical transduction as well as optical monitoring. The advantage of this strategy resides in the fast and easy surface modification with the targeting ligands. Therefore, the functionalized surface was combined with cell-on-a-chip systems to monitor living cells and the effects of drugs and chemicals by optical and also electrochemical detection.

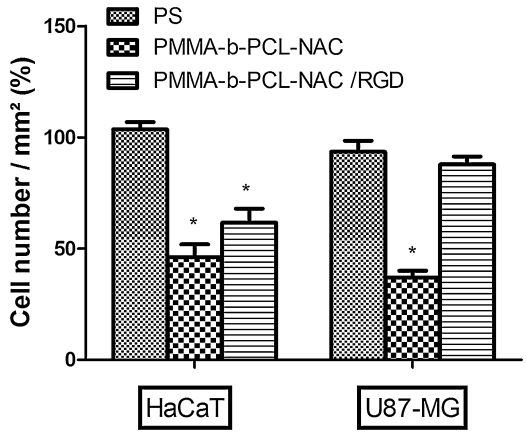

Figure 7. Number of HaCaT and U87-MG cell lines after 72 h incubation on control polystyrene, PMMA-b-PCL-NAC, and PMMA-b-PCL-NAC-RGD surfaces ($n = 3$). Error bars mean the ± SD. Asterisks indicate the differences compared to the PS surface for both of the cell line.

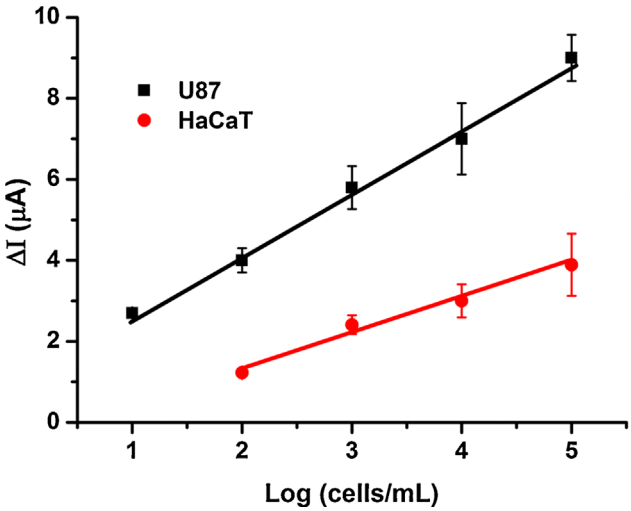

Figure 8. Linearity curves of GCE/ PMMA-b-PCL-NAC-RGD/U87-MG and GCE /PMMA-b-PCL-NAC-RGD /HaCaT electrodes [measurements were carried out via DPV technique related to the difference of currents that was mentioned in material and method and in the presence of 10.0 mM, $[Fe(CN)_6]^{-3/-4}$ within PBS buffer, pH 7.4. Error bars mean the ± SD ($n = 3$)].

5. Appendix/Nomenclature/Abbreviations

NAC	N-acetyl-L-cysteine
PCL	polycaprolactone
PLA	poly(lactic acid)
PLGA	poly(lactideco-glycotide)
PMMA	poly(methyl methacrylate)
PMMA-*b*-PCL-NAC	N-acetyl-L-cysteine-capped poly-(methyl methacrylate)-*b*-polyca-prolactone block copolymer
CuAAC	copper catalyzed azide–alkyne cycloaddition
RGD	arginylglysylaspartic acid
PMMA-*b*-PCL-NAC-RGD	RGD-modified PMMA-*b*-PCL-NAC
EDC	1-ethyl-3-(3 dimethylaminopro-pyl) carbodiimide
THF	tetrahydrofuran
ECM	extracellular matrix
αvβ	alpha V beta 3
MTT	3-(4,5-dimethylthiazol-2-yl)-2,5-diphenyltetrazolium bromide
DAPI	4′,6-diamidino-2 phenylindole
PBS	phosphate-buffered saline
GCEs	glassy carbon electrodes
Pt	platinum
DPV	differential pulse voltammetry
CV	cyclic voltammetry

Acknowledgements: This project was supported by the Scientific and Technological Research Council of Turkey (TUBITAK, project number 113Z918) and the Ege University Research Foundation (14-FEN-023). EGE University, AREL Central Laboratory is acknowledged for the flow cytometry analyses. Authors also thank IYTE MAM for SEM analyses. The authors of this work would also like to acknowledge and thank TÜBİTAK for the 2236 Co-Funded Brain Circulation Scheme (Co-Circulation scheme), partially supported by the EC-FP7 Marie Curie Actions-People-COFUND and coordinated by BİDEB as a source of funding.

Received: March 21, 2015; Revised: April 21, 2015; Published online:DOI: 10.1002/mabi.201500099

Keywords: cell adhesion; cell sensing; electrochemical biosensor; selective surfaces

[1] E. Primiceri, M. S. Chiriacò, R. Rinaldi, G. Maruccio, *Lab Chip* **2013**, *13*, 3789.
[2] P. Wang, Q. Liu, *Cell-Based Biosensors: Principles and Applications*, Artech House, MA, USA **2009**, p. 271.
[3] J. El-Ali, P. K. Sorger, K. F. Jensen, *Nature* **2006**, *442*, 403.
[4] R. Langer, D. A. Tirrell, *Nature* **2004**, *428*, 487.
[5] F. B. Barlas, D. Ag Seleci, M. Ozkan, B. Demir, M. Seleci, M. Aydin, M.A. Tasdelen, H. M. Zareie, S. Timur, S. Ozcelik, Y. Yagci, *J. Mater. Chem. B* **2014**, *2*, 6412.
[6] P. Neirynck, J. Schimer, P. Jonkheijm, L-G. Milroy, P. Cigler, L. Brunsveld, *J. Mater. Chem. B* **2014**, *3*, 539.
[7] S. R. Meyers, M. W. Grinstaff, *Chem. Rev.* **2012**, *112*, 1615.
[8] Y. Zhu, C. Gao, X. Liu, J. Shen, *Biomacromolecules* **2002**, *3*, 1312.
[9] H. C. Kolb, M. G. Finn, K. B. Sharpless, *Angew. Chem. Int. Ed. Engl.* **2001**, *40*, 2004.
[10] C. W. Tornøe, C. Christensen, M. Meldal, *J. Org. Chem.* **2002**, *67*, 3057.
[11] C. E. Hoyle, C. N. Bowman, *Angew. Chem. Int. Ed. Engl.* **2010**, *49*, 1540.
[12] a) D. Bacinello, E. Garanger, D. Taton, K. C. Tam, S. Lecommandoux, *Eur. Polym. J* **2015**, *62*, 363. b) K. Bury, F. Du Prez, D. Neugebauer, *Macromol. Biosci.* **2013**, *13*, 1520. c) S. M. Brosnan, H. Schlaad, *Polymer* **2014**, *55*, 5509. d) B. Dervaux, F. E. Du Prez, *Chem. Sci.* **2012**, *3*, 959. e) M. A. Tasdelen, Y. Yagci, *Angew. Chem. Int. Ed.* **2013**, *52*, 5930. f) S. Doran, Y. Yagci, *Polym. Chem.* **2015**, *6*, 946. g) E. Murtezi, Y. Yagci, *Macromol. Rapid Commun.* **2014**, *35*, 1782. h) A. B. Lowe, *Polym. Chem.* **2010**, *1*, 17.
[13] S. Doran, E. Murtezi, F. B. Barlas, S. Timur, Y. Yagci, *Macromolecules* **2014**, *47*, 3608.
[14] G. Oyman, C. Geyik, R. Ayranci, M. Ak, D. Odaci Demirkol, S. Timur, H. Coskunol, *RSC Adv.* **2014**, *4*, 53411.
[15] R. A. D'Sa, P. J. Dickinson, J. Raj, B. K. Pierscionek, B. J. Meenan, *Soft Matter* **2011**, *7*, 608.
[16] J. Yang, D. H. Kim, J. L. Hendricks, M. Leach, R. Northey, D. C. Martin, *Acta Biomater.* **2005**, *1*, 125.
[17] Polymers for Regenerative Medicine, C. Werner, Ed., *Advances in Polymer Science*, Vol. *203*, Springer, Berlin, Heidelberg **2006**.
[18] D. Liu, C. A. Che Abdullah, R. P. Sear, J. L. Keddie, *Soft Matter* **2010**, *6*, 5408.
[19] U. Geissler, U. Hempel, C. Wolf, D. Scharnweber, H. Worch, K. Wenzel, *J. Biomed. Mater. Res.* **2000**, *51*, 752.
[20] Y. Takada, X. Ye, S. Simon, *Genome Biol.* **2007**, *8*, 215.
[21] B. Alberts, A. Johnson, J. Lewis, M. Raff, K. Roberts, P. Walter, *Molecular Biology of the Cell*, 5st ed., Garland Science, Taylor & Francis Group, LLC, NewYork, USA **2008**, p. 1170.

[22] A. R. Hsu, A. Veeravagu, W. Cai, L. C. Hou, V. Tse, X. Chen, *Recent Pat. Anticancer Drug Discov.* **2007**, *2*, 143.
[23] Z. Liu, F. Wang, X. Chen, *Drug Dev. Res.* **2008**, *69*, 329.
[24] B. Felding-Habermann, T. E. O'Toole, J. W. Smith, E. Fransvea, Z. M. Ruggeri, M. H. Ginsberg, P. E. Hughes, N. Pampori, S. J. Shattil, A. Saven, B. M. Mueller, *Proc. Natl. Acad. Sci. USA* **2001**, *98*, 1853.
[25] C. R. Cooper, C. H. Chay, K. J. Pienta, *Neoplasia* **2002**, *4*, 191.
[26] R. Soldi, S. Mitola, M. Strasly, P. Defilippi, G. Tarone, F. Bussolino, *EMBO J.* **1999**, *18*, 882.
[27] S. M. Albelda, S. A. Mette, D. E. Elder, R. Stewart, L. Damjanovich, M. Herlyn, C. A. Buck, *Cancer Res.* **1990**, *50*, 6757.
[28] S. Zitzmann, V. Ehemann, M. Schwab, *Cancer Res.* **2002**, *62*, 5139.
[29] F. Danhier, A. Le Breton, V. Préat, *Mol. Pharm.* **2012**, *9*, 2961.
[30] S. Regis, S. Youssefian, M. Jassal, M. Phaneuf, N. Rahbar, S. Bhowmick, *Polym. Eng. Sci.* **2014**, *54*, 2587.
[31] T. A. Petrie, J. E. Raynor, C. D. Reyes, K. L. Burns, D. M. Collard, A. J. García, *Biomaterials* **2008**, *29*, 2849.
[32] M. S. Tjin, A. W. C. Chua, D. R. Ma, S. T. Lee, E. Fong, *Macromol. Biosci.* **2014**, *14*, 1125.
[33] T. A. Petrie, J. E. Raynor, D. W. Dumbauld, T. T. Lee, S. Jagtap, K. L. Templeman, D. M. Collard, A. J. Garcia, *Sci. Transl. Med.* **2010**, *2*, 45.
[34] L. Qu, J. Xu, X. Tan, Z. Liu, L. Xu, R. Peng, *ACS Appl. Mater. Interfaces* **2014**, *6*, 7309.
[35] G. T. Hermanson, *Bioconjugate Techniques*, 3rd edition, Academic Press, London, UK **2013**, p. 127.
[36] K. Matyjaszewski, *Macromolecules* **2012**, *45*, 4015.
[37] T. Cai, M. Li, B. Zhang, K-G. Neoh, E-T. Kang, *J. Mater. Chem. B* **2014**, *2*, 814.
[38] I. Javakhishvili, S. Hvilsted, *Biomacromolecules* **2009**, *10*, 74.
[39] H. Wu, H. Chen, Y. Sun, Y. Wan, F. Wang, B. Jia, X. Su, *Cancer Lett.* **2013**, *335*, 75.
[40] Y. Wu, X. Zhang, Z. Xiong, Z. Cheng, D. R. Fisher, S. Liu, S. S. Gambhir, X. Chen, *J. Nucl. Med.* **2005**, *46*, 1707.
[41] H. Wang, K. Chen, W. Cai, Z. Li, L. He, A. Kashefi, X. Chen, *Mol. Cancer Ther.* **2008**, *7*, 1044.